Eur. Phys. J. A (2012) **48**: 151
DOI 10.1140/epja/i2012-12151-1

THE EUROPEAN PHYSICAL JOURNAL A

Letter

The size of the proton: Closing in on the radius puzzle

I.T. Lorenz[1,a], H.-W. Hammer[1,b], and Ulf-G. Meißner[1,2,c]

[1] Helmholtz-Institut für Strahlen- und Kernphysik and Bethe Center for Theoretical Physics, Universität Bonn, D-53115 Bonn, Germany
[2] Institute for Advanced Simulation and Jülich Center for Hadron Physics, Institut für Kernphysik, Forschungszentrum Jülich, D-52425 Jülich, Germany

Received: 23 October 2012
Published online: 6 November 2012

Communicated by E. De Sanctis

Abstract. We analyze the recent electron-proton scattering data from Mainz using a dispersive framework that respects the constraints from analyticity and unitarity on the nucleon structure. We also perform a continued fraction analysis of these data. We find a small electric proton charge radius, $r_E^p = 0.84^{+0.01}_{-0.01}$ fm, consistent with the recent determination from muonic hydrogen measurements and earlier dispersive analyses. We also extract the proton magnetic radius, $r_M^p = 0.86^{+0.02}_{-0.03}$ fm, consistent with earlier determinations based on dispersion relations.

The proton charge radius is a fundamental quantity of physics. It is truly remarkable that, despite decade-long experimental and theoretical efforts, its precise value is not yet determined. The recent controversy about the size of the proton was triggered by the precision measurement of the Lamb shift in muonic hydrogen that led to a "small" charge radius, $r_E^p = 0.84184(67)$ fm [1]. This result came as a big surprise as it was in stark contrast to the commonly accepted "large" CODATA value of 0.8768(69) fm [2], based on the measurements of the Lamb shift in electronic hydrogen and the analysis of electron-proton scattering data. The large value was further strengthened by the high-precision electron-proton scattering measurements at MAMI-C [3, 4]. The analysis of these data including two-photon corrections led to $r_E^p = 0.876(8)$ fm. These authors also found a magnetic radius of the proton that came out much smaller than commonly accepted values, $r_M^p = 0.803(17)$ fm.

On the theoretical side, a precise *ab initio* calculation based on lattice QCD is not yet available due to various conceptual problems to be overcome like the treatment of disconnected contributions that feature importantly in isoscalar quantities. See, *e.g.*, [5] for a recent work. A different framework, that was pioneered by Höhler and collaborators a long time ago, are dispersion relations (DRs) for the nucleon electromagnetic form factors [6]. In such type of approach, smaller radii were always favored, and the most recent and sophisticated DR calculation led to values consistent with the ones from muonic hydrogen, $r_E^p = 0.844^{+0.008}_{-0.004}$ fm [7]. The value for the proton's magnetic radius was $r_M^p = 0.854 \pm 0.005$ fm, consistent with, *e.g.*, the determination based on continued fractions by Sick [8]. Note, however, that the conformal mapping technique to analyze the nucleon form factors led to a large value of the proton charge radius [9].

Given this puzzling situation, in this letter we will re-analyze the MAMI data of Bernauer *et al.* [3] using dispersion relations. Our main focus will be on the correct treatment of the analytical structure of the nucleon form factors that is driven by the two-pion continuum. Its important role was already stressed by Frazer and Fulco, who were able to predict the ρ-resonance and its influence on the nucleons' structure a long time ago [10]. What has often been overlooked since this seminal work was the large enhancement of the two-pion continuum on the left wing of the ρ-resonance due to a close-by pole on the second Riemann sheet in the elastic pion-nucleon scattering amplitude. This enhancement amounts for roughly half of the nucleon isovector size [6]. This important effect is also recovered in chiral perturbation theory, the effective field theory of QCD at low energies [11]. We consider it, therefore, of utmost importance to include this effect in the re-analysis of the MAMI data. Of course, in light of the muon $g-2$ measurement at BNL [12], one might speculate about the influence of new physics as the muon data are more sensitive to such effects, but first one has to exclude possible conventional explanations —and we will offer such a possibility here.

[a] e-mail: lorenzi@hiskp.uni-bonn.de
[b] e-mail: hammer@hiskp.uni-bonn.de
[c] e-mail: meissner@hiskp.uni-bonn.de

The nucleon matrix element of the electromagnetic current,

$$\langle N(p')|j_\mu^{\rm em}|N(p)\rangle = ie\bar{u}(p')\left(\gamma_\mu F_1(t) + i\frac{\sigma_{\mu\nu}q^\nu}{2m_N}F_2(t)\right)u(p), \quad (1)$$

is parameterized in terms of the Dirac, $F_1(t)$, and Pauli, $F_2(t)$, form factors, with $t = (p'-p)^2 = -Q^2$ the invariant momentum transfer squared, and m_N is the nucleon mass. For the electron-nucleon scattering, we have $Q^2 \geq 0$. $F_1^{p/n}(0)$ and $F_2^{p/n}(0)$ are given in terms of the proton/neutron electric charge and anomalous magnetic moment, respectively. For the later analysis, it is useful to separate the form factors in their isoscalar and the isovector parts, $F_i^s = (F_i^p + F_i^n)/2$ and $F_i^v = (F_i^p - F_i^n)/2$ for $i = 1, 2$, correspondingly. The differential cross-section is given most compactly in terms of the Sachs form factors $G_E(t) = F_1(t) - \tau F_2(t)$, $G_M(t) = F_1(t) + F_2(t)$, with $\tau = -t/4m_N^2$, so that

$$\frac{{\rm d}\sigma}{{\rm d}\Omega} = \left(\frac{{\rm d}\sigma}{{\rm d}\Omega}\right)_{Mott}\frac{\tau}{\epsilon(1+\tau)}\left[G_M^2(Q^2) + \frac{\epsilon}{\tau}G_E^2(Q^2)\right], \quad (2)$$

where $\epsilon = [1+2(1+\tau)\tan^2(\Theta/2)]^{-1}$ is the virtual photon polarization, Θ is the electron scattering angle in the laboratory frame, and $({\rm d}\sigma/{\rm d}\Omega)_{Mott}$ is the Mott cross-section, which corresponds to scattering on a point-like particle. The electric and magnetic radii of the proton, that are in the focus of this Letter, are given by

$$r_{E,M}^p = \left(\frac{-6}{G_{E,M}(0)}\frac{{\rm d}G_{E,M}(Q^2)}{{\rm d}Q^2}\bigg|_{Q^2=0}\right)^{1/2}. \quad (3)$$

To analyze the cross-section data from Mainz based on eq. (2), we use unsubtracted dispersion relations for the nucleon form factors. For a generic form factor in the space-like region, these take the form

$$F(t) = \frac{1}{\pi}\int_{t_0}^{\infty}\frac{{\rm Im}F(t'){\rm d}t'}{t'-t}, \quad (4)$$

with $t_0 = 4M_\pi^2\,(9M_\pi^2)$ the pertinent isovector (isoscalar) threshold and M_π is the charged pion mass. The basic quantity in this relation is the spectral function ${\rm Im}F(t)$ that parameterizes all physical effects that contribute to the nucleon form factors. The most general form of the spectral function allowed by unitarity is a sum of continua and poles. This is exactly the form of the spectral function we use in our analysis. The low-mass continua $(2\pi, K\bar{K}, \rho\pi)$ are included exactly, whereas higher-mass continua are approximated by effective vector meson poles.

In our DR approach, the complete isoscalar and isovector parts of the Dirac and Pauli form factors, respectively, are parameterized as

$$F_i^s(t) = \sum_{V=K\bar{K},\rho\pi,s_1,s_2,\ldots}\frac{a_i^V}{m_V^2-t},$$
$$F_i^v(t) = \sum_{V=v_1,v_2,\ldots}\frac{a_i^V}{m_V^2-t} + \frac{a_i + b_i(1-t/c_i)^{-2}}{2(1-t/d_i)}, \quad (5)$$

where $i = 1, 2$. Each pole term comes, in principle, with three parameters —the two residua and the mass. While the low-mass pole terms can be interpreted as physical vector mesons, *i.e.* the ω and the ϕ, the higher-mass poles are effective poles that parameterize unknown continuum contributions. The residua for the light vector mesons ω, ϕ are related to more or less known coupling constants, see, *e.g.*, ref. [7] for a detailed discussion. Therefore, we constrain the residua of the light isoscalar vector mesons as: $0.5\,{\rm GeV}^2 < |a_1^\omega| < 1\,{\rm GeV}^2$, $|a_2^\omega| < 0.5\,{\rm GeV}^2$ [13] and $|a_1^\phi| < 2\,{\rm GeV}^2$, $|a_2^\phi < 1\,{\rm GeV}^2$ [14]. Additional poles below $1\,{\rm GeV}^2$ can be excluded since no other vector mesons exist in this region. At higher masses, the widths get broader and with growing distance to the space-like region their position cannot be resolved precisely. Therefore this part of the spectral function can only be described by effective pole terms. Besides the vector meson pole terms, our DR approach includes the two-pion continuum, the $K\bar{K}$ and $\rho\pi$ continua. The two latter contributions to the form factors are also parameterized by pole terms with fixed masses and residua, as was done before, see refs. [14–16]. The last term in eq. (5) is an appropriate parameterization of the two-pion continuum, that also includes the ρ pole as discussed above. The parameters are

$$a_1 = 1.084, a_2 = 5.800, b_1 = 0.079, b_2 = 0.751,$$
$$c_1 = 0.300\,{\rm GeV}^2, c_2 = 0.225\,{\rm GeV}^2,$$
$$d_1 = 0.522\,{\rm GeV}^2, d_2 = 0.562\,{\rm GeV}^2.$$

Note that this parameterized form of the low-mass continua is only used for faster numerical evaluations. The total number of isoscalar and isovector poles is determined from the stability criterion of ref. [**?**], which in a nutshell can be described as using the lowest numbers of parameters that are required to obtain a good fit to the data. The superconvergence relations enforcing the correct asymptotic power behavior of the form factors,

$$\int_{t_0}^{\infty}{\rm Im}\,F_i(t)\,t^n\,{\rm d}t = 0, \quad i = 1, 2, \quad (6)$$

with $n = 0$ for F_1 and $n = 0, 1$ for F_2, are included as well.

With this DR ansatz, we reconstruct the differential cross sections and fit to the MAMI data for ep scattering and simultaneously to the world data for the neutron form factors. The fits are done in the one-photon approximation via the Rosenbluth formula where the data contains most of the higher-order corrections [3]. However, the Coulomb corrections are replaced in our analysis by a better approximation as was done by [18]. For a recent discussion on this point, see refs. [4, 19]. We remark that two-photon exchange corrections are expected to be small for the charge radius extraction, see, *e.g.*, refs. [20, 21], but somewhat more sizeable for the magnetic radius [4, 22]. This requires further study.

We fit to the Mainz data floating the normalization of the individual data sets by at most $\pm 4\%$ (in most cases this normalization change is less than 1%), using the 31 normalization parameters given in ref. [23]. Employing the aforementioned stability criterion, we include

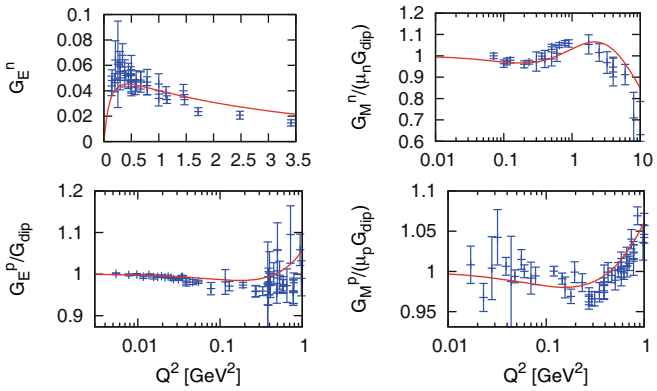

Fig. 1. Form factors from our dispersion relation analysis in comparison to world form factor data as given by [7] (updated to include also the more recent data [24]).

Table 1. Fit parameters from dispersion analysis (cf. eq. (5)). Masses m_V are given in GeV and couplings a_i^V in GeV^2.

V	m_v	a_1^V	a_2^V	V	m_V	a_1^V	a_2^V
ω	0.783	0.747	0.003	v_1	1.205	0.826	−2.557
ϕ	1.019	0.221	−0.014	v_2	2.140	−0.502	0.438
s_1	1.638	0.977	0.234	v_3	1.000	−0.381	−0.342
s_2	2.400	−0.501	−0.077	v_4	1.193	−0.227	0.831
s_3	1.033	−0.540	−0.333				

5 isoscalar and 4 isovector resonances with in total 15 additional parameters. We impose the constraints from the normalizations, from the superconvergence relations and the fact that the masses of the lowest isoscalar poles, the $\omega(782)$ and the $\phi(1020)$ are known. For details of the fitting procedure, see ref. [7]. This fit gives a good description of the proton cross-section and neutron form factor data with $\chi^2_{\rm red} = 2.2$. The form factors arising from this fit are shown in fig. 1. The corresponding fit parameters are given in table 1. The obtained residua of ω and ϕ are in agreement with their couplings to the nucleon, as described above. All remaining poles have residua with natural size. Varying the number of pole terms in both isospin channels does not affect the radii significantly but is included in our error estimate.

To address the issue of the theoretical uncertainties of our analysis, we vary the isovector and isoscalar continuum contributions in all possible combinations and repeat the fit to obtain the corresponding ranges. The two-pion continuum is varied by 5% below the first minimum of the pion-nucleon scattering amplitudes and 20% above it. We note that at present a Roy-Steiner machinery is set up to improve the representation of the t-channel pion-nucleon phase shifts required here [25], but for our investigation we use an updated version of the two-pion continuum representation from Ref. [26], including new data for the pion vector form factor from KLOE [27] and BABAR [28]. The error in the two-pion continuum from the difference between the KLOE and BABAR data sets is well below the assigned 5–20% uncertainty. It is also important to note that the Roy-Steiner analysis of ref. [25] has shown that

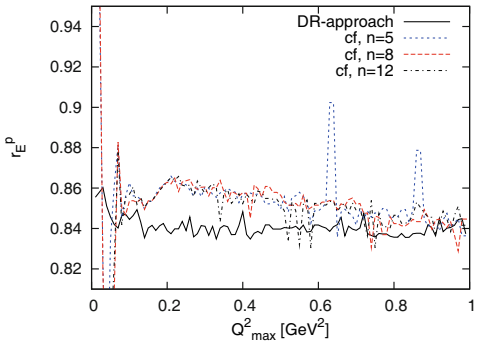

Fig. 2. Dependence of the proton electric radius r_E^p on $Q^2_{\rm max}$ for CF fits. Here, n labels the number of terms. For comparison, the DR approach is also shown.

the KH80 solution used here is internally consistent. The $K\bar{K}$ and $\rho\pi$ continua are varied by 20%. We have also varied the number of effective pole terms and obtained stable results.

The extracted proton radii are:

$$r_E^p = 0.84^{+0.01}_{-0.01}\,\text{fm}, \qquad r_M^p = 0.86^{+0.02}_{-0.03}\,\text{fm}. \tag{7}$$

For the neutron magnetic radius, we obtain $r_M^n = 0.88 \pm 0.05\,\text{fm}$, consistent with previous analyses. The neutron electric radius is very insensitive to the variation of the continua. We obtain the value $(r_E^n)^2 = -0.127\,\text{fm}^2$. To examine the influence of the neutron data, we also fit the DR model exclusively to the electron-proton scattering cross-sections. The effect on the proton radii is less than half a percent on the numbers given above. If the superconvergence relations, eq. (6), are not enforced, the same radii are obtained within the quoted uncertainties.

To assess the stability of the results obtained, we make use of a continued fraction (CF) approach as advocated, *e.g.*, by Sick [18]. Every rational function can be represented by a general continued fraction function and in contrast to a polynomial, this can generate poles. Therefore it can well approximate the data beyond the threshold where the imaginary part sets in. We fit the following inverse CF ansatz [18]:

$$F(t) = \cfrac{1}{1 + \cfrac{f_1 t}{1 + \cfrac{f_2 t}{1 + \ldots}}} \tag{8}$$

to our data, in order to examine under which circumstances and how exactly the generation of isolated poles suffices to simulate the so important two-pion continuum contribution. In particular, we have investigated the dependence of the fits on the highest value of Q^2 (denoted $Q^2_{\rm max}$ from here on) for which data is included. This dependence can be used to demonstrate the need to include imaginary parts in the fit functions and include data beyond the two-pion threshold to obtain a stable fit. The electric radius derived from such fits shows only small fluctuations for varying $Q^2_{\rm max}$, as shown in fig. 2. For the magnetic radius, we do not find stable results with varying number of continued fractions and thus will not

consider it any more. Remarkably, the electric radius of the proton show large fluctuations in the CF approach for $Q^2_{\rm max} \leq 0.1\,{\rm GeV}^2$, but then converges quickly towards values consistent with the ones based on the theoretically preferable DR approach. These results might at first appear surprising, as naively a low $Q^2_{\rm max}$ might be favored, because the relevant information for the radius extraction is related to the region of small momentum transfer. On the other hand, the uncertainty due to the normalization has obviously a stronger influence on the radius for lower Q^2. The less stable values at very low $Q^2_{\rm max}$ in the DR approach might be explained by this normalization uncertainty or simply by an insufficient amount of data. At higher values of $Q^2_{\rm max}$ the fluctuations in the derived radii increase. We assume that this is due to an insufficient number of free fit parameters for more data since the fluctuations are stronger for lower n. Increasing the data range also increases the $\chi^2_{\rm red}$ slightly. Of course, this could either show the inability of the models to describe the data at higher momentum transfers or it could be due to a bad estimation of errors in this data. We cannot separate these effects, which may both apply here: i) it is obvious that the fit functions are only approximate and ii) the errors of the data are scaled to yield a $\chi^2_{\rm red} \approx 1$ for a spline fit and thus contain a model dependence [23]. Therefore, the χ^2 values or confidence limits are not used to weight the extracted radii. The results are weighted equally and only the spikes of the fits with $\chi^2_{\rm red} \simeq 1.7$ are omitted, less than 3 for each set of results. The remaining $\chi^2_{\rm red}$ values for all fits with $Q^2_{\rm max} \geq 0.1\,{\rm GeV}^2$ vary, *e.g.*, for the CFs of order 5 between $\chi^2_{\rm red} = 1.03$ and 1.64. The average and standard deviation of the radius values extracted for $Q^2_{\rm max}$ between $0.1\,{\rm GeV}^2$ and the complete data set range up to $0.98\,{\rm GeV}^2$ are $r_E^p = 0.85 \pm 0.01\,{\rm fm}$ for $n = 5$, $n = 8$ and $n = 12$ (to obtain these results, we have utilized the improved Coulomb corrections as described before). These numbers are in good agreement with the values obtained via the DR approach and the recent muonic hydrogen measurements. We are presently studying the application of the conformal mapping technique of Hill and Paz [9] to the MAMI data to further sharpen our conclusion on the value of the proton charge radius [29].

In this letter, we have reconsidered the proton radii determination from the new MAMI electron-proton scattering data, using two very different methods. First, we have used a dispersive representation of the nucleon form factors that includes the so important constraints from unitarity and analyticity —these were not considered in the fit functions utilized in refs. [3,4]. Including also data from the world data set on the neutron form factors, we achieve a good description of the cross-section data. We have also performed an analysis of the systematic uncertainties by allowing for generous variations in the $\pi\pi$, $\bar{K}K$ and $\pi\rho$ contributions to the spectral functions. The resulting electric and magnetic radii, cf. eq. (7) are in stark contrast to the ones obtained in refs. [3,4], but our results are consistent with all earlier dispersive analyses of the nucleon form factors [7, 30–32]. Also, the small value for r_E^p is consistent with the recent muonic hydrogen measurement [1]. We have also applied the continuous fraction method to the data. By construction, it can emulate narrow poles but to account for the so important two-pion continuum, one has to choose a sufficiently large fit range, $Q^2_{\rm max} \geq 0.1\,{\rm GeV}^2$, to achieve stable results. Again, this method leads to values for the proton charge radius in agreement with the dispersive approach. We conclude that the small proton electric radius is indeed favored if analyticity and unitarity are properly included into the description of the nucleon electromagnetic form factors.

We thank M. Distler and I. Sick for discussions and A. Denig for providing the pion form factor data. This work is supported in part by the DFG and the NSFC through funds provided to the Sino-German CRC 110 "Symmetries and the Emergence of Structure in QCD", and the EU I3HP "Study of Strongly Interacting Matter" under the Seventh Framework Program of the EU, and by BMBF (Grant No. 06BN7008).

References

1. R. Pohl *et al.*, Nature **466**, 213 (2010).
2. P.J. Mohr, B.N. Taylor, D.B. Newell, Rev. Mod. Phys. **80**, 633 (2008) arXiv:0801.0028 [physics.atom-ph].
3. A1 Collaboration (J.C. Bernauer *et al.*), Phys. Rev. Lett. **105**, 242001 (2010) arXiv:1007.5076 [nucl-ex].
4. J.C. Bernauer *et al.*, Phys. Rev. Lett. **107**, 119102 (2011).
5. S. Collins *et al.*, Phys. Rev. D **84**, 074507 (2011) arXiv:1106.3580 [hep-lat].
6. G. Höhler, E. Pietarinen, Phys. Lett. B **53**, 471 (1975).
7. M.A. Belushkin, H.-W. Hammer, U.-G. Meißner, Phys. Rev. C **75**, 035202 (2007) hep-ph/0608337.
8. I. Sick, Prog. Part. Nucl. Phys. **55**, 440 (2005).
9. R.J. Hill, G. Paz, Phys. Rev. D **82**, 113005 (2010) arXiv:1008.4619 [hep-ph].
10. W.R. Frazer, J.R. Fulco, Phys. Rev. Lett. **2**, 365 (1959).
11. V. Bernard, N. Kaiser, U.-G. Meißner, Nucl. Phys. A **611**, 429 (1996) hep-ph/9607428.
12. Muon G-2 Collaboration (G.W. Bennett *et al.*), Phys. Rev. D **73**, 072003 (2006) hep-ex/0602035.
13. W. Grein, P. Kroll, Nucl. Phys. B **137**, 173 (1978).
14. U.-G. Meißner, V. Mull, J. Speth, J.W. van Orden, Phys. Lett. B **408**, 381 (1997) hep-ph/9701296.
15. H.-W. Hammer, M.J. Ramsey-Musolf, Phys. Rev. C **60**, 045204 (1999) **62**, 049902(E) (2000) hep-ph/9903367.
16. H.-W. Hammer, M.J. Ramsey-Musolf, Phys. Rev. C **60**, 045205 (1999) **62**, 049903(E) (2000) hep-ph/9812261.
17. I. Sabba Stefanescu, J. Math. Phys. **21**, 175 (1980).
18. I. Sick, Phys. Lett. B **576**, 62 (2003) nucl-ex/0310008.
19. J. Arrington, Phys. Rev. Lett. **107**, 119101 (2011) arXiv:1108.3058 [nucl-ex].
20. P.G. Blunden, I. Sick, Phys. Rev. C **72**, 057601 (2005) nucl-th/0508037.
21. M.A. Belushkin, H.-W. Hammer, U.-G. Meißner, Phys. Lett. B **658**, 138 (2008) arXiv:0705.3385 [hep-ph].

22. J. Arrington, arXiv:1210.2677 [nucl-ex].
23. J.C. Bernauer, PhD thesis, Johannes Gutenberg-Universität Mainz (2010).
24. S. Riordan *et al.*, Phys. Rev. Lett. **105**, 262302 (2010) arXiv:1008.1738 [nucl-ex].
25. C. Ditsche, M. Hoferichter, B. Kubis, U.-G. Meißner, JHEP **06**, 043 (2012) arXiv:1203.4758 [hep-ph].
26. M.A. Belushkin, H.-W. Hammer, U.-G. Meißner, Phys. Lett. B **633**, 507 (2006) hep-ph/0510382.
27. KLOE Collaboration (F. Ambrosino *et al.*), Phys. Lett. B **700**, 102 (2011) arXiv:1006.5313 [hep-ex].
28. BABAR Collaboration (B. Aubert *et al.*), Phys. Rev. Lett. **103**, 231801 (2009) arXiv:0908.3589 [hep-ex].
29. I.T. Lorenz, H.-W. Hammer, U.-G. Meißner, in preparation.
30. G. Höhler, E. Pietarinen, I. Sabba Stefanescu, F. Borkowski, G.G. Simon, V.H. Walther, R.D. Wendling, Nucl. Phys. B **114**, 505 (1976).
31. P. Mergell, U.-G. Meißner, D. Drechsel, Nucl. Phys. A **596**, 367 (1996) hep-ph/9506375.
32. H.-W. Hammer, U.-G. Meißner, Eur. Phys. J. A **20**, 469 (2004) hep-ph/0312081.